7
Co Substituted Z-Type Sr Hexaferrite and its Composites for 8-18 GHz MW Absorption

7.1 INTRODUCTION

Magnetic materials like barium or strontium hexaferrites have attracted attention due to the strong anisotropy and moderate magnetization, suitable for numerous applications including microwave absorption. The different morphological microstructures can be produced by varying the synthesis conditions and therefore different physical properties can be obtained within the same crystallographic phase. Barium and Strontium hexaferrites are hexagonal crystal structures and the schematic structure with preferred c-axis orientation, is shown in Figure 7.1(a). The compositions of these hexaferrites are guided by the ternary phase diagram, shown in Figure 7.1(b). The hard ferrite phase is marked as M and other known phases are indicated by the respective symbols with different stoichiometric composition of Ba, MeO and Fe_2O_3. The respective chemical compositions of these phases have been discussed in chapter 2.

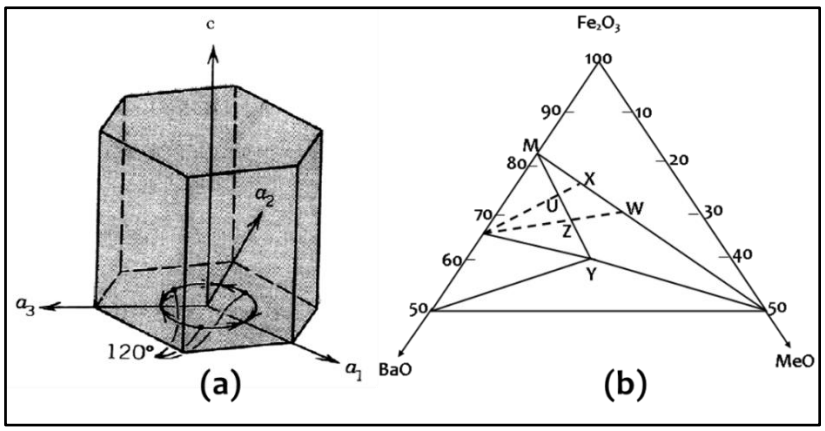

Figure 7.1 : (a) Hexagonal lattice cell (b) Part of the phase diagram BaO-MeO-Fe_2O_3, where Me is divalent metal ion of Mn, Fe, Co, Ni, Zn or Mg etc. [Source: Pullar, 2012]

The Co substituted Z-type Sr hexaferrite ($Sr_3Co_2Fe_{24}O_{41}$/Sr_3Co_2Z) shows spontaneous magnetization in the direction of basal plane, perpendicular to c-axis and make them potential candidate for MW absorption [Puller, 2012]. The actual crystal structure of Z-phase is quite complex, where number of different oxides can be formed, depending on how the close-packed layers are stacked. In this structure, close-packed Barium/Strontium (II) and oxide ions are large and Iron (III) ions are located at their interstices. The typical crystal structure of Z-type Sr hexaferrite, which is combination of M and Y-phase hexaferrite phases, is shown in Figure 7.2. The crystal structure of Z-type hexaferrite can be explained by superposition of layers of R, S and T blocks. The atomic arrangement of S ($2SrFe_2O_4$), R ($SrFe_6O_{11}$) and T ($Sr_2Fe_8O_{14}$) blocks in Z-type Sr hexaferrite are shown in Figure 7.2. Further, R*, S* and T* are the representation for 180° angle rotated R, S and T blocks respectively, along c-axial direction.

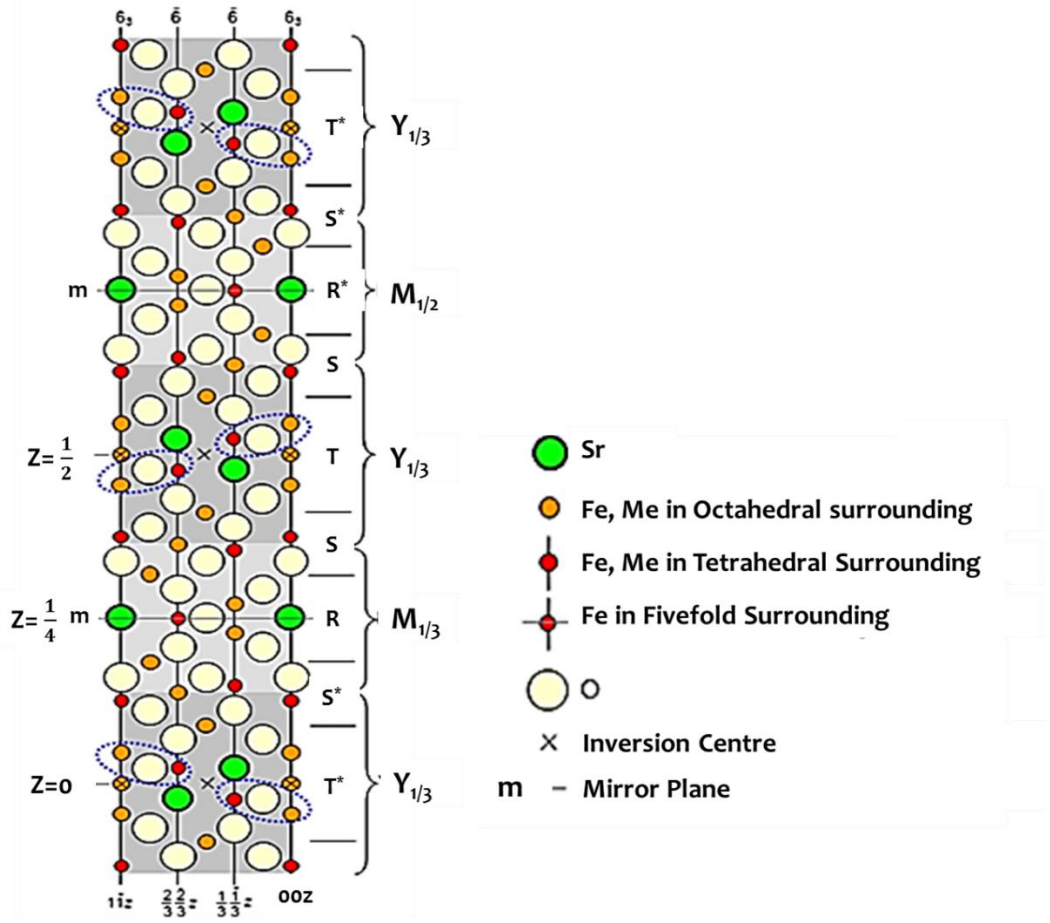

Figure 7.2: Crystal Structure of Z-type Hexaferrites ($Sr_3Co_2Fe_{24}O_{41}$) (Source: Scott, 2013)

MW absorption properties in hexaferrites are primarily governed by ferromagnetic resonance (FMR) relaxation and structure dependent anisotropic effects. FMR relaxation in ferrite has been already discussed in chapter 2 and 4 for MW absorption. Magnetic anisotropy has its origin in sample's shape and size, crystalline symmetry, stress or preferential atomic pair ordering for a given material. The physical origin of magnetocrystalline anisotropy is relies on low symmetry crystal field and a nonzero spin-orbit interaction in the crystal. If the atomic orbital has zero angular moment (L_z=0) , such as Fe^{3+} and Mn^{2+}, it does not matter what the symmetry of the crystal field is; the orbital can take any orientation with respect to the crystal. If the orbitals have nonzero angular momentum <$L_Z \neq 0$>, such as $Co^{2+}$and Fe^{2+}, only certain orientations will be preferred in crystal fields of lower symmetry. Therefore, Co^{2+} and Fe^{2+} ions have more contribution to the magnetocrystalline anisotropy than Fe^{3+} and Mn^{2+} due to the nonzero orbital angular moment. According to the easy magnetization directions, Sr_3Co_2Z hexaferrite has c-plane anisotropies. There are six easy magnetization directions separated by angles of 60° from each other in the c-plane as shown in Figure 7.3. They lie along the crystallographic directions of [0 1 -1 0], [-1 1 0 0] and [0 -1 1 0]. When external EM/magnetic fields are applied, the magnetization vectors can be rotated from one easy magnetization direction to another easy magnetization direction in the c-plane, following the external stimuli. The corresponding magnetic fields driving the rotation of magnetic vector can be defined as out-of-plane anisotropy field H_θ and in-plane anisotropy field H_φ. The energy required to rotate the magnetization from the easy direction to another direction is called magnetocrystalline anisotropy energy, which can be expressed in terms of certain anisotropy constants and the direction to which the magnetization is rotated. The magntocrystalline energy E can be expressed by the following Eq. (7.1)

$$E = K_0 + K_1 Sin^2\theta + K_2 Sin^4\theta + K_3 Sin^6\theta \, Cos6\Phi + \ldots. \quad (7.1)$$

Where, K_0 is energy required to magnetize the materials in easy axis, K_1, K_2 and K_3… are the first, second and third…order magnetocrystalline anisotropy constants, respectively. For c-plane anisotropy, $K_1+K_2 < 0$, and the anisotropy field H_θ and H_φ can be expressed as given in Eq. (7.2) and (7.3) [Puller, 2012].

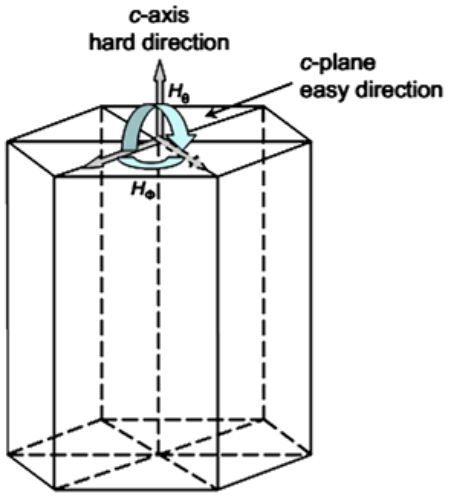

Figure 7.3 : C-planer anisotropy in Sr_3Co_2Z hexaferrite

$$H_\theta = -\frac{2\,(K_1+2K_2)}{M_s} \tag{7.2}$$

$$H_\Phi = \frac{36\,K_3}{M_s} \tag{7.3}$$

The value of anisotropy filed can be easily estimated from the data of anisotropy constants and saturation magnetization. The crystalline anisotropy can be changed over a large range of values by the substituting the transition metal ions by divalent ions with different ionic radii. It has been observed that Co^{2+} has strong contribution to planar anisotropy due to its negative contribution to the first order magnetocrystalline anisotropy constant K_1 [Pullar, 2012]. Therefore, the substitution of Co ions modifies the anisotropy from c-axis to c-plane for W, Z-ferrites, and increase the c-plane anisotropy for Y-ferrite. For such systems, the FMR frequency depends highly on anisotropy parameters as given by Eq. (7.4) [Pullar, 2012]

$$f_r = \frac{\gamma}{2\pi}\sqrt{H_\theta H_\Phi} \tag{7.4}$$

The shape and morphology of the particulates play important factor in the microwave absorption properties, for example, hexaferrites with platy morphologies exhibit enhanced microwave absorption with respect to other crystallite morphology. This is because of the effective propagation path of the microwave, which can be much larger in anisotropic medium than in the isotropic one, thus resulting in more effective absorption. Further, spin re-orientation perpendicular to the crystallographic plane leads to the better absorption in hexaferrites with preferred directions. In this context, the development of platy morphology for the particles is highly desirable. The Sr_3Co_2Z materials are found in hexagonal shaped platy morphology, which makes this system a suitable candidate for MW absorbing applications. However, the biggest challenge is the synthesis/preparation of pure Z-phase hexaferrite materials. The earlier studies indicate that there is a possibility of formation of phase pure Sr_3Co_2Z material along with residual M, W, Y hexaferrite phases. Further, pure phase material has been obtained in narrow annealing temperature window (1225°C-1275°C) with large annealing time periods and also the low yields of the end product [Grunberger *et al.*, 1991]. In the present chapter, an innovative synthesis route has been established to overcome these issues and provide an improved, simple, cost effective, time savings, energy efficient method for the preparation of Z-type hexaferrite in large quantity.

The synthesized materials show good magnetic loss in broad microwave frequency range of 8-18 GHz.

7.2 EXPERIMENTAL PROCEDURE

The detailed process steps, for preparation of Z-type hexaferrtie (Sr_3Co_2Z), are explained in Figure 7.4. Initially, aqueous solutions of metal salts e.g. Strontium chloride ($SrCl_2.6H_2O$, CAS No. 10025-70-4), Iron (III) chloride anhydrate ($FeCl_3$, CAS No. 7705-08-0) and Cobalt chloride ($CoCl_2.6H_2O$, CAS No. 7791-13-1) were prepared in proper stoichiometry. The mixing of metal salt solutions was carried out using magnetic stirrer continuously for 10-15 minutes. The mixed solution was then slowly heated to 110-120°C at 3-4°C/minutes heating rate and kept for 15-20 minutes under continuous stirring. The precipitation of metal salt was carried out by adding drop wise 1M Sodium Carbonate (Na_2CO_3, CAS No. 497-19-8) solution into aqueous mixture until the pH of final solution reached ~9. The precipitated material was separated using vacuum filtration and washed using hot distilled water to remove the residual chloride ions entrapped in precipitate. The resultant precipitate was dried in oven at ~85-100°C temperature range for 6h. The dried lumped powder was crushed and ground to make the fine powder of the synthesized material. The dried powder was subjected to critical heat treatments at different temperatures for the formation of phase pure ferrite material. Initially, powder was annealed in air for 4h at ~650°C with 10°C/minute heating rate and cooled down to the room temperature. The powder thus, obtained from this process was further annealed at ~ 950°C for 3h in air ambient at 8°C/minute heating rate and cooled down to room temperature at free rate. The annealing process has increased the particle size from fine nano precipitated powder to sub-micron regime. The final powder was homogenized further by crushing and grinding to obtain the uniformly distributed final product. The powder was further annealed at temperature of 1250°C for 3h at relatively slow heating rate ~5°C/minute and cooled down to room temperature in normal conditions. In this process, ferrite particles grow larger to micron range. The final powder, thus obtained after this process, was crushed in mixture-cum-grinder and sieved through 100 μm mesh size sieve to collect the powder having uniform particle distribution. The process described above can produce large quantity of pure cobalt substituted Z-phase strontium hexaferrite powder.

Rubber based composites were fabricated by impregnating 1250°C annealed Sr_3Co_2Z ferrite powder at different 50-80wt% loading fraction in NBR rubber matrix, as mentioned in Table 7.1. The 50, 60, 70, and 80wt% hexaferrite loaded rubber samples were designated as ZSR50, ZSR60, ZSR70, and ZSR80 respectively, for later discussion. All the composite samples were prepared in the form ~2 mm thick sheets. EM parameters of these SCZ-rubber composites were measured using wave guide transmission line technique in X-band (8-18 GHz) and Ku-band (12.4-18 GHz) of the MW spectrum. The reflection loss (R.L.) values were calculated using the measured EM parameters for all these composites for different absorber thicknesses.

Table 7.1: List of Sr_3Co_2Z ferrite loaded rubber composites

S. No.	Sample Code	Quantity of NBR (g)	Wt% of Sr_3Co_2Z ferrite in compound	Quantity of ferrite powder (g)	Enhancement in filler loading as compared to sample ZSR50 (x)
1	ZSR50	20	50	20	1.00
2	ZSR60	20	60	30	1.50
3	ZSR70	20	70	46.7	2.33
4	ZSR80	20	80	80	4.00

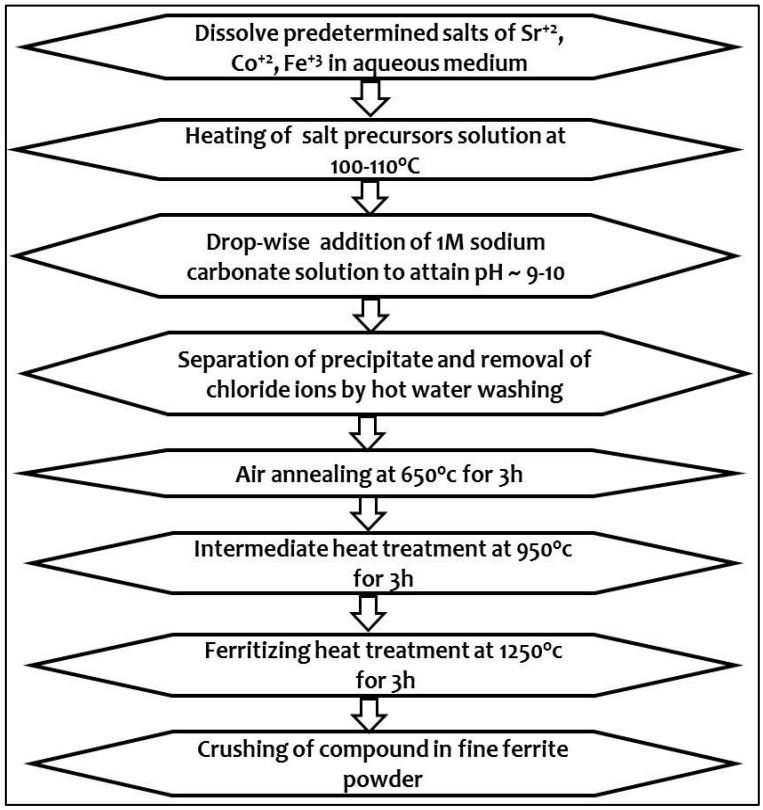

Figure 7.4 : Process flow chart for synthesis of microwave absorbing Z-type hexaferrite powder

High temperature resistant sintered tiles are practically being used for different applications viz. aircraft exhaust, ground radar's floor area, anechoic chambers etc. to get the broad band MW absorption at lesser absorber thickness, as these are purely made by functional material itself without any matrix/ingredient. However, for MW absorption applications, ferrite/ceramic oxide based tiles are more feasible because of high impedance mismatch problem in the dielectric materials based tiles. In the present thesis work, attempts were made to fabricate hexaferrite based sintered tiles to achieve 8-18 GHz absorption application at lesser thickness as compared to that of spinel ferrites. In the present chapter, Sr_3Co_2Z ferrite powder based sintered tiles were prepared to evaluate their MW absorption properties. The process of fabricating sintered tiles is shown in Figure 7.5.

Initially, identified ferrite powder with maximum MW absorption properties (Z-type Sr ferrite) was mixed with 10% Poly Vinyl Alcohol (PVA) solution in a granulator (Model: EL1, Make: EIRICH, Germany) as shown in Figure 7.5. The ferrite/PVA mixture was converted into PVA coated granules of size ~10-20 mm. Granulation of ferrite powder is essential for uniform filling of ferrite material into the die sets of hydraulic press. Moreover, during the granulation process, uniform coating of PVA on ferrite materials improves the binding properties of ferrite particulates. The high capacity automatic hydraulic press (Model: VPM 120 SC, Make: LAUFFER Inc., Germany) with ~300 Ton pressing capacity was used for compaction of ferrite powder. The ferrite granules were transferred into 10 cm x 10 cm die set for hydraulic press. Ferrite material was compacted with 1Ton/cm^2 pressure for green body formation. The desired thickness of green body is obtained by adjusting the depth of die slot for filling of the required quantity of ferrite granules.

The ferrite green body was sintered at high temperature with sintering cycle, as shown in Figure 7.6 to achieve the mechanical strength. Initially, the green body was heated at 250°C for 1 hour at the heating rate of 2°C/min to burn out the PVA content. Subsequently, the sintering temperature was raised to 1250°C at the heating rate of ~1.4°C/min and kept for 3h for curing of the tiles. After this process, furnace was cooled down to room temperature under normal ambient

conditions. During this high temperature sintering process, porosity among ferrite granules has reduced and mechanical strength has increased of these ferrite tiles. The obtained sintered tile was characterized for its MW absorption properties over 8-18 GHz frequency range

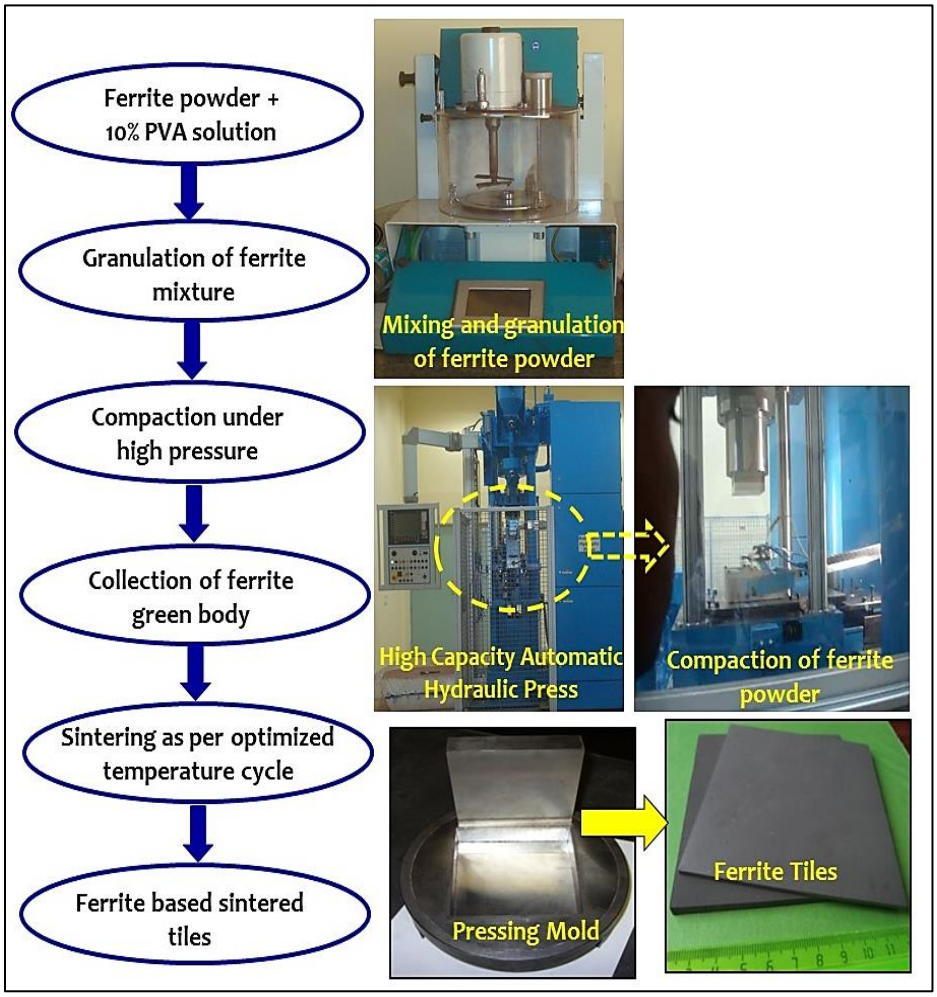

Figure 7.5 : Process flow chart for fabrication of microwave absorbing ferrite tiles

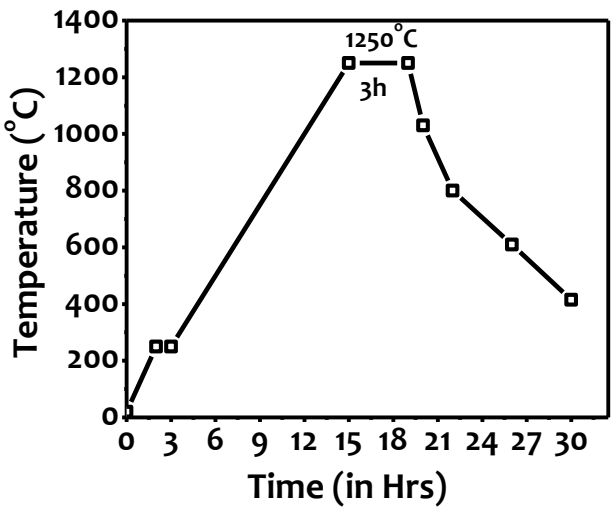

Figure 7.6 : Typical sintering cycle for treatment of ferrite tiles

7.3 RESULTS AND DISCUSSIONS

7.3.1 X-ray Diffraction Analysis

The optimization of heat treatment process has been monitored using X-ray diffraction (XRD) measurements to get pure Z-phase and intermediate hexaferrite phases by annealing at different temperatures. The XRD spectra for 950°C, 1250°C, and 1350°C annealed Sr_3Co_2Z powders are shown in Figure 7.7, with respective heating profile. The 950°C heat treated sample showed M-phase hexaferrite material with $SrFe_{12}O_{19}$ stoichiometric composition. The M-phase is considered to be the most energetically favored hexaferrite phase, formed at relatively lower heating temperature [Zhang *et al.*, 2001]. The heating of M-phase materials at 1250°C for 3h converted it directly into pure Z-phase without any secondary phase. The XRD peaks, observed at 2θ ~30.4°, ~32.6° and ~35.1° corresponding to (1 1 0), (1 0 16), and (1 1 10) planes respectively [ICDD card No. 019-0097], confirmed the formation of pure Z-phase hexaferrite.

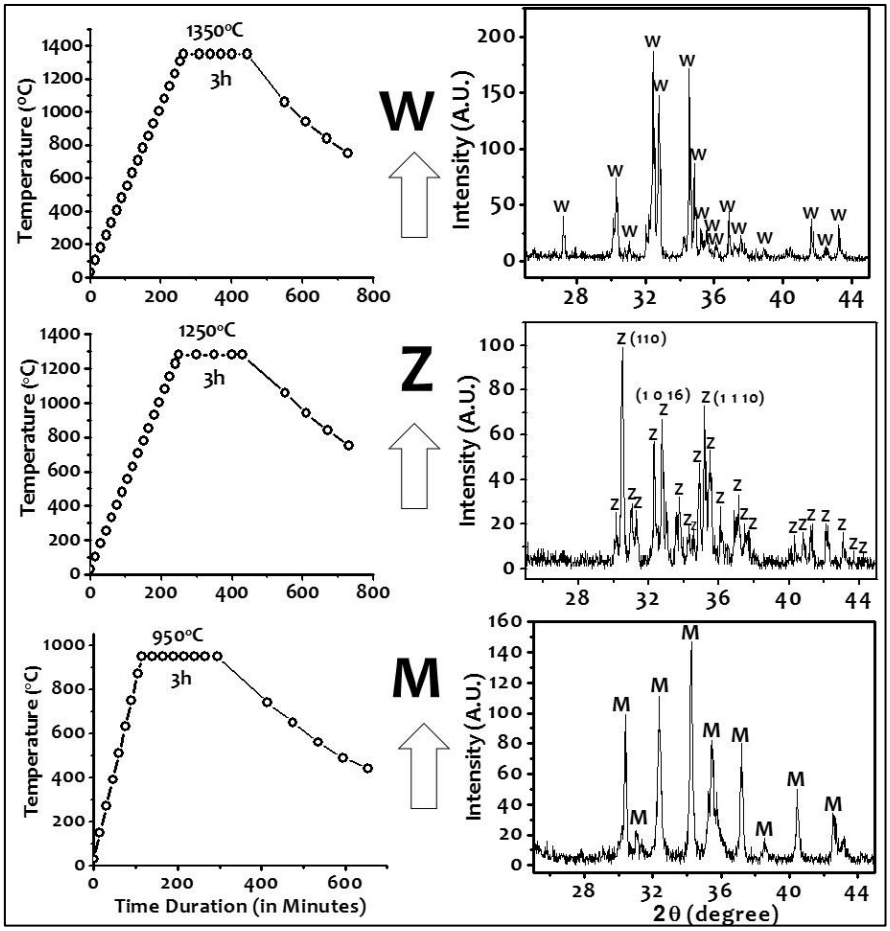

Figure 7.7 : Annealing temperature profile and corresponding X-ray diffraction patterns for different M, Z and W phase hexaferrite powders

In the present study, formation of intermediate M-phase is found to be excellent precursor material for conversion of pure Z-phase hexaferrite without any residual phases, also consistent with similar reports [Pullar and Bhattacharya, 2001]. Therefore, in the present synthesis route, intermediate heating of ferrite powder at 950°C is an essential steps for formation of pure Z-phase. To study the effect of temperature on Z-phase, the sample was further annealed at 1350°C for 3h with heating rate of ~5°C/minute. Interestingly the Z-phase has converted into pure W-phase hexaferrite, as can be inferred from the respective XRD spectra. Hence, with increasing the annealing temperature, Z-phase ($Sr_3Co_2Fe_{24}O_{41}$) hexaferrite can be completely decomposed into W-phase ($SrCo_2Fe_{16}O_{27}$), which is stable at higher temperatures.

7.3.2 Morphological Analysis

SEM micrographs at different magnifications are collected and shown in Figures 7.8(a)-(c) for 1250°C annealed Sr_3Co_2Z hexaferrite powder sample. These observations suggest the platy morphology with distorted hexagonal structures for Z hexaferrite sample. The particle size distribution was measured by laser based particle size analyzer (Model: S3500, Make: Microtrac). The size of particles found in the range of 1-20 µm with average particle size ~10 µm, as shown in Figure 7.9. These studies indicate that the present synthesis method, utilized for the formation of pure Z- phase hexaferrite, provide narrow distribution of particle size in the micron range.

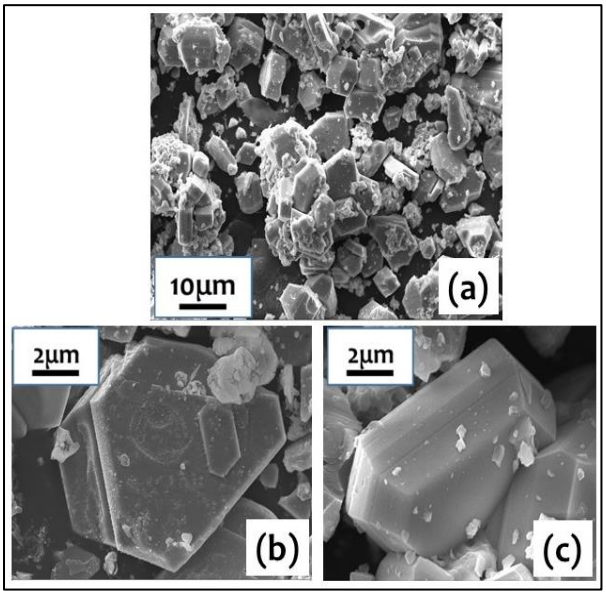

Figure 7.8 : SEM micrographs for Sr_3Co_2Z hexaferrite powder annealed at 1250°C for different magnifications

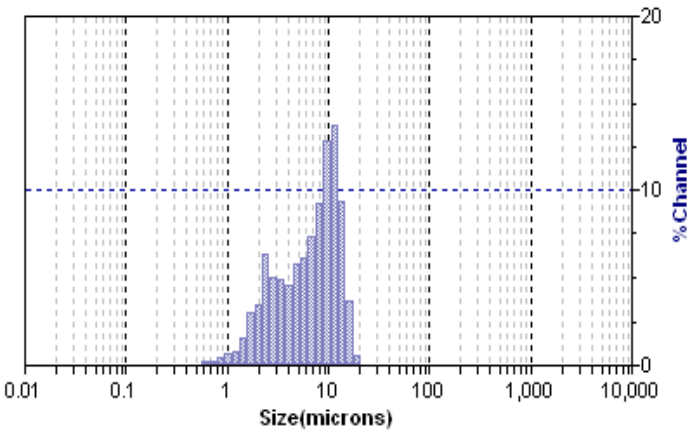

Figure 7.9 : Particle size distribution for Sr_3Co_2Z hexaferrite powder annealed at 1250°C

7.3.3 Magnetic Studies

The room temperature M-H hysteresis measurements were recorded for 950°C, 1250°C and 1350°C annealed hexaferrite samples in the magnetic field range -1.5T to +1.5T. The magnetographs are shown in Figures 7.10(a)-(c). The hysteresis curves show ferromagnetic behavior for all these ferrite samples. The powder annealed at 950°C shows saturation magnetization value (M_s) ~88 emu/g with coercive field value ~2.5K Oe. The observed value of coercive field is significantly high due to c-axis anisotropy in the M-phase hexaferrite sample without any divalent metal ions except iron [Shams *et al.*, 2008]. Further, the saturation magnetization is ~96 emu/g, with coercive field value ~80 Oe, for 1250°C annealed Z-type

hexaferrite powder sample. The enhancement in the magnetization values in Z-type hexaferrites may be attributed to the cobalt magnetic ions and their more complex arrangements/interactions within Z-type crystal atomic layers. In this phase, the magnetization increases sharply with applied magnetic field in the range of -2KOe to +2KOe. This behavior ensures the quick magnetic ordering of domains under the influence of external magnetic field, and thus, resulting into the lower values of coercive field [Ghasemi *et al.*, 2006]. The observed low coercive field value in this phase is due to the change of magnetization from c-axis easy magnetization to the basal plane of hexaferrite. This change of c-axis anisotropy to c-plane anisotropy has reduced the magneto-crystalline anisotropy in the system [Kagotani *et al.*, 2004; Ruan *et al.*, 2000]. The powder annealed at 1350°C shows the saturation magnetization M_s ~79 emu/g with coercive field value ~87 Oe. The observed lower saturation magnetization value for W phase as compared to the Z-phase is because of the crystallographic arrangement of magnetic ions and their complex interaction. However, coercive field value are in the same range ~87 Oe and is attributed to c-plane anisotropy nature of the W-phase with Co substitution [Qin *et al.*, 2013].

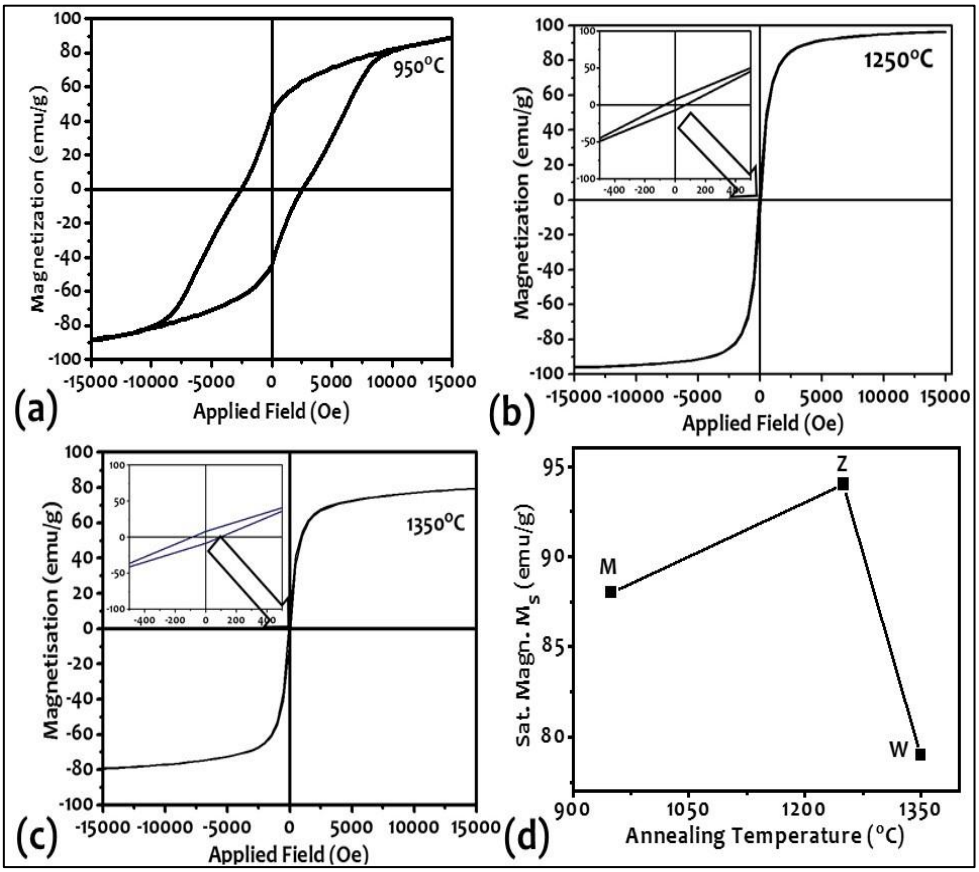

Figure 7.10 : Room temperature M-H hysteresis curves for Sr_3Co_2Z hexaferrite powder annealed at (a) 950°C (b) 1250°C (c) 1350°C, and (d) variation of saturation magnetization with annealing temperature

7.3.4 Microwave Studies

Complex permittivity and permeability values of ferrite powders annealed at 950°C (M-phase), 1250°C (Z-phase), and 1350°C (W-phase) were measured using a wave guide transmission line method over the frequency range of 8-18 GHz. Real permittivity (ε_r') values are shown in Figure 7.11(a) for different ferrite phases in 8-18 GHz frequency range. The real permittivity values for M-phase lie in the range of ~10.2 to ~9.3 for 8-18 GHz frequency range with a decreasing trend towards higher frequency. These observed values are consistent with earlier reports [Narang and Hudiara, 2006; Tyagi, 2011]. However, for Z-phase, ε_r' values are in the range ~13.5 to ~12.9 for 8-18 GHz frequency range. The increase in ε_r' values is attributed to the inter-conversion of Fe^{3+} ions to Fe^{2+} ions at higher annealing temperature [Abdullah and Yusoff, 1997]. Similarly, real values of W-phase are found in the range of ~12.6 to 11.6 over 8-18 GHz frequency

range. The similar frequency dispersion characteristics are observed for all these different hexaferrite phases. The imaginary permittivity (ε_r'') values for all these three phases are negligible in 8-18 GHz frequency range and therefore not presented here.

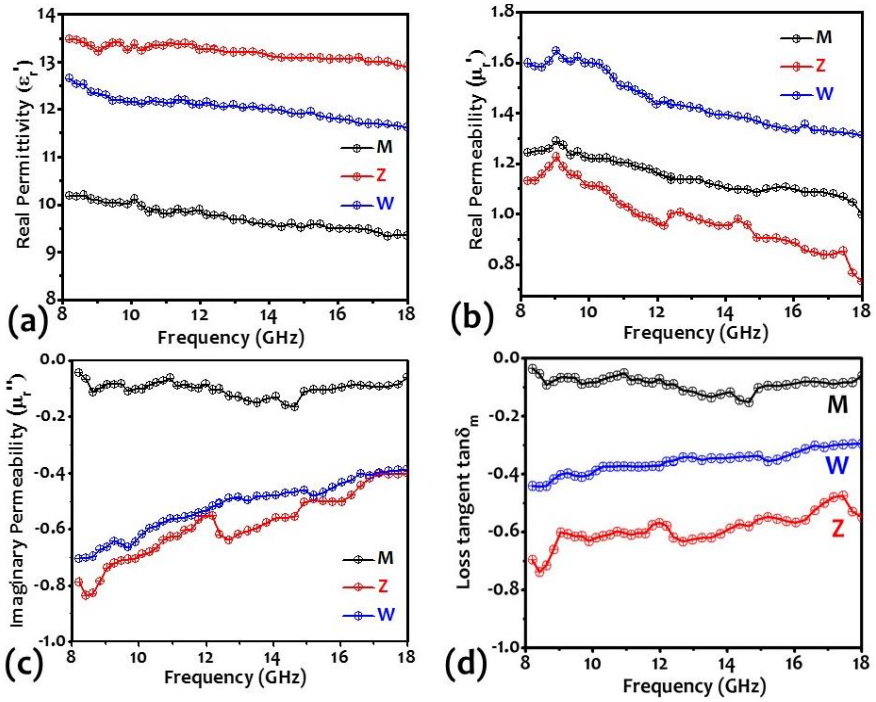

Figure 7.11 : Frequency dependence of (a) Real permittivity (ε_r') (b) Real permeability (μ_r') (c) Imaginary permeability (μ_r'') (d) Loss tangent ($\tan\delta_m$) for hexaferrite powder samples annealed at 950°C, 1250°C, and 1350°C

The real permeability (μ_r') values are observed in the range of ~1.25 to ~1.0 for M phase hexaferrite, with a decreasing trend towards higher frequencies, as shown in Figure 7.11(b). These values for Z-phase are found in the range of ~ -1.15 to -0.75 over 8-18 GHz with a similar trend. However, for W-phase, the real permeability values increased significantly and lie in the range of ~ -1.6 to -1.3 over 8-18 GHz. As per the Snoek's relation $f(\mu_r-1)=4/3\pi M_s$, the decrease in real permeability value at a particular frequency can be correlated to saturation magnetization (M_s) value of the materials [Snoek, 1946]. The higher saturation magnetization value for Z-phase as compared to M-phase has resulted into lower real permeability value for Z-phase hexaferrite material. The significant increase in values of W-phase is due to sharp decrease in M_s value to ~79 emu/g with respect to Z-phase (~96 emu/g). Moreover, the density of ferrite materials increases with increasing annealing temperature, which also enhances the spin magnetic moments per unit volume and thus, enhanced real permittivity values, as observed in the present study [Zhang *et al.*, 2003]. The imaginary permeability (μ_r''), which influences the MW absorption properties of materials, is increased with increasing annealing temperatures. The imaginary permeability (μ_r'') values of M-phase are ~ -0.10 with negligible frequency dispersion as shown in Figure 7.11(c). The low values of μ_r'' in M-phase hexaferrite have been observed and are attributed to the high coercive field values for this phase, as the spins are unable to follow the EM field. However, in Z-phase hexaferrite μ_r'' values are found in the range of ~ -0.80 to ~ -0.40, over the frequency range ~8-18 GHz. The higher μ_r'' values indicate that the effective contribution of planar anisotropy of Z-type hexaferrite in MW absorption process. In this case, spin re-orientation from hard plane to c-axis requires more energy and thereby, enhanced microwave absorption. Further, μ_r'' values for W-phase are decreased slightly as compared to Z-phase, and values lie in the range ~ -0.7 to ~ -0.4 over 8-18 GHz frequency range. This may be due to the decomposition of high magnetized phase (Z) to less magnetized W phase, and thus, leading to the less interaction of MW radiation with ferromagnetic domains. The calculated magnetic loss tangent ($\tan\delta_m = \mu_r''/\mu_r'$) values are shown in the Figure 7.11(d) for these different phase hexaferrite samples. The magnetic loss

tangent ($\tan\delta_m$) values for M, Z, and W-phase hexaferrite materials are found in the range of ~ -0.1 to -0.06, ~ -0.7 to -0.5, and ~-0.44 to -0.30, respectively. The higher values of $\tan\delta_m$ in Z-phase are attributed to the lower values of μ_r' and higher values of μ_r'' among all these three phases. This material (Z-type hexaferrite) was selected for fabricating rubber composite based EM absorbers, as explained in section 7.2.

Real part of permittivity (ε_r') values for Z-type hexaferrite powder loaded composite rubber samples (ZSR50-ZSR80) are shown in Figure 7.12(a). The permittivity values for all these composite samples are almost constant with negligible frequency dispersion characteristics in 8-18 GHz frequency range. The ε_r' values for ZSR50, ZSR60, ZSR70, and ZSR80 are ~3.5, ~4.2, 5.1, and ~6.5, respectively. The observed enhancement in ε_r' values, with increasing the loading fraction of ferrite powder, indicates the larger contribution of ferrite powder in composite rubber samples. The real permeability (μ_r') values for rubber based composites found to be increased with loading fraction of ferrite material as shown in Figure 7.9(b). The μ_r' values for ZSR50, ZSR60, ZSR70, and ZSR80 rubber composites lie in the range of ~ 1.04 to 0.92, ~ 1.06 to 0.96, ~ 1.13 to 0.98, and ~ 1.21 to 1.03, respectively. Further, the variation of imaginary permeability (μ_r'') values with frequencies are shown in Figure 7.12(c).

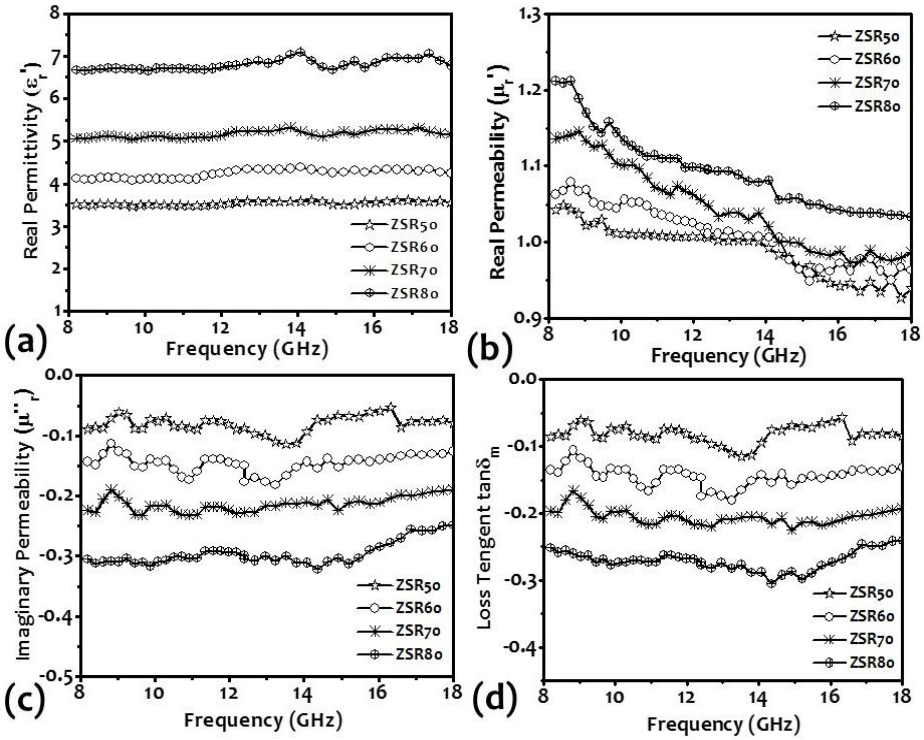

Figure 7.12 : Frequency dependence of (a) Real permittivity (ε_r') (b) Real permeability (μ_r') (c) Imaginary permeability (μ_r'') (d) Loss tangent ($\tan\delta_m$) for Z-type hexaferrite powder loaded rubber samples ZSR50-ZSR80

The μ_r'' values have increased from ~ -0.1 to -0.3 for sample from ZSR50 to ZSR80. Three times enhancement have been observed in μ_r'' values after increasing the loading fraction from 50 to 80wt%. The similar behavior of ε_r', μ_r' and μ_r'' with frequencies in ferrite loaded rubber based composites have been reported earlier [Abbas *et al.*, 2007; Gama and Rezende, 2013; Vinayasree *et al.*, 2014]. The magnetic loss tangent ($\tan\delta_m$) values are shown in Figure 7.12(d) for all ferrite loaded rubber samples. The largest values of $\tan\delta_m$ observed are ~ -0.25 for ZSR80 composite sample in the entire 8-18 GHz frequency range.

The thickness dependent reflection loss (R.L.) values are plotted in Fig. 7.13 for all ferrite loaded samples (ZSR50-ZSR80) over 8-18 GHz frequency range. Sr_3Co_2Z ferrite powder loaded rubber sample with 50wt% concentration showed negligible R.L. values due to the insufficient interaction of MW signals with functional filler material. With further increase in loading fraction of ferrite material to 60 and 70wt%, the R.L. values increased almost identically for both these

samples. The optimum matching thickness of absorbers for these loading is ~2.2 mm with maximum reflection loss $(R.L.)_{max.}$ ~7 dB at ~13 GHz frequency. The R.L. values are still insignificant for practical application for these absorbers. Further, gain in R.L. values was observed at higher ferrite loading of 80wt% in conjunction with the thickness dependent resonating behavior. The optimal reflection loss $(R.L.)_{max.}$ value observed is ~11 dB at matching thickness of ~2.0 mm and ~ 13 GHz frequency for ZSR80 composite sample.

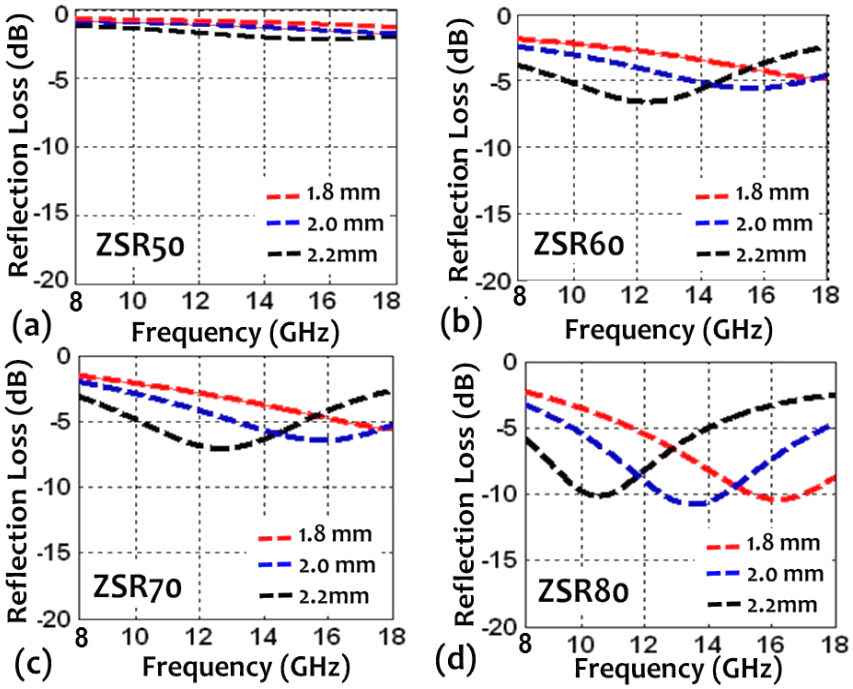

Figure 7.13 : Optimal Reflection Loss (R.L.) over frequency range 8-18 GHz and matching thicknesses of ferrite loaded rubber composites (a) ZSR50 (b) ZSR60 (c) ZSR70 (d) ZSR80

The complex EM parameters of Z-phase ferrite, shown in Figure 7.11 were used, for computing the R.L. values for hexaferrite based sintered tiles. The thickness dependent R.L. plots are shown in Figure 7.14 (a) in the range of 1-1.8 mm of the ferrite tile. The R.L. values for ferrite tiles are relatively larger as compared to that of rubber composite based MW absorbers, due to the enhanced MW interaction with ferrite material present with 100% loading in ferrite tiles. At the tile thickness of 1.2 mm, the R.L. values are found > 10 dB over 11.5-18 GHz (Absorption band width ~6.5 GHz) with maximum values ~23 dB at ~15 GHz. At the tile thickness of 1.4 mm, the resonance behavior was observed with frequency bandwidth of 8.5 GHz, showing $(R.L.)_{max}$ value ~43 dB at ~12.5 GHz. This is because of the close impedance matching at $\lambda_m/4$ thickness. With further increase in tile thickness to 1.6 mm, maximum R.L. value has reduced to ~28 dB while the absorption bandwidth has increased to ~9.5 GHz. Further increase in tile thickness beyond 1.6mm, neither provides any significant gain in (R.L.) values nor in the absorption bandwidth. The Figure 7.14(b) shows the variation of absorption bandwidth and maximum reflection loss values $(R.L.)_{max}$ as a function of ferrite tile thickness. These observations suggest that 1.4 mm thick tile can be considered for optimal (R.L.) performance without much compromise with absorption bandwidth. Moreover, the thickness of tiles can be tuned as per the desired central frequency of MW absorption for different applications.

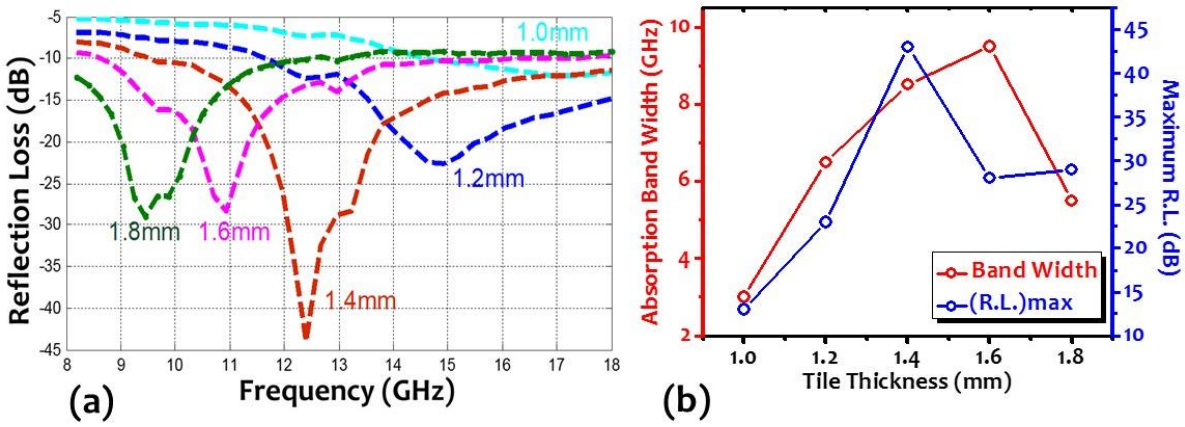

Figure 7.14 : (a) Thickness dependent (R.L.) values of Sr_3Co_2Z ferrite sintered tile (b) Variation of MW absorption bandwidth and maximum (R.L.) values with thickness of ferrite tile

7.4 CONCLUDING REMARKS

An optimized process has been designed and developed to produce Co substituted Z-type Sr hexaferrite with desired coercive field and saturation magnetization in conjunction with effective magnetic tangent loss over wider 8-18 GHz microwave frequency range. The method for producing hexagonal ferrite includes the stoichiometric weights of required metal salts as the starting materials and followed by precipitating with carbonate ions in aqueous medium. Further, three stage heat treatment process has been established and optimized in narrow temperature zone to produce the pure phase Z-type hexagonal ferrite materials. The ferrite powder produced by this process exhibits important physical parameters desired for microwave energy absorption in the frequency range 8-18 GHz. The ferrite materials, prepared by this process, exhibit very good magnetic loss ($\tan\delta_m > 0.5$) over the frequency range of 8-18 GHz, which may result in enhanced microwave energy absorption. The filler loaded rubber composite (ZSR50-ZSR80) samples have been developed, which showed enhancement in (R.L.) values with increasing the loading fraction of hexaferrite material in rubber matrix. The ferrite based tiles showed excellent MW absorption ~43 dB over a wider frequency band of 9.5-18 GHz at relatively lesser thickness ~ 1.4 mm. Thus ferrite based tiles can be used in wider band MW absorbing application without much implication of weight and thickness of the absorbers.

...